Energy 86 (2015) 59–73

Contents lists available at ScienceDirect

Energy

journal homepage: www.elsevier.com/locate/energy

Organic Rankine cycle saves energy and reduces gas emissions for cement production

Huarong Wang, Jinliang Xu*, Xufei Yang, Zheng Miao, Chao Yu

The Beijing Key Laboratory of Multiphase Flow and Heat Transfer, North China Electric Power University, Beijing 102206, China

ARTICLE INFO

Article history:
Received 27 August 2014
Received in revised form
9 February 2015
Accepted 25 March 2015
Available online 15 May 2015

Keywords:
Organic Rankine cycle
Cement
Waste heat
Economic performance
Environment impact

ABSTRACT

We investigated ORCs (organic Rankine cycles) integrated with typical China cement production line. The dry air at the kiln cooler outlet with the temperature of 220 °C was the waste heat. The fluids of hexane, isohexane, R601, R123 and R245fa were selected for ORCs based on the critical temperature criterion. The developed ORC verified the thermodynamics analysis. The NPV (net present value) and PBP (payback period) methods were applied to evaluate the economic performance. The LCA (life cycle assessment) was applied to evaluate the environment impacts. ORCs could generate 67,85,540–81,21,650 kWh electricity per year, equivalent to save 2035–2436 tons standard coal and reduce 7743–9268 tons CO_2 emission, for a 4000 t/d cement production line. ORCs reduced gas emissions of CO_2 by 0.62–0.74%, SO_2 by 3.83–4.59% and NO_x by 1.36–1.63%. The PBP (payback period) was 2.74–3.42 years. The ORCs had the reduction ratios of EIL (environment impact load) by 1.49–1.83%, GWP (global warming potential) by 0.74–0.92%, AP (acidification potential) by 2.34–2.84%, EP (eutrophication potential) by 0.96–1.22% and HTP (human toxicity potential) by 2.38–2.89%. The ORC with R601 as the fluid had the best economic performance and significant gas emission reductions. ORCs had good economic performance and reduce the gas emissions.

1. Introduction

The cement industry is a basic raw material industry to influence a country's economy and people's life. It has attained a considerable scale in China. The annual output of cement was about 2414 million tons, accounting for about 60% of the world's cement output in 2012 [1]. There are large quantities of low grade waste heat during the cement production process. As the second largest waste heat resource among the seven industry sectors of steel, cement, glass, synthetic ammonia, caustic soda, calcium carbide, sulphuric acid, the waste heat in the cement industry was equivalent to 93 million tons standard coal in China [2]. The waste heat driven power generation technologies have evolved three generations in the cement industry. The available power generation technologies use relatively high grade waste heat. The water-vapor Rankine cycle was used, with the vapor temperature higher than 370 °C. The power generation system is complicated and the investment cost is high [3].

Recently, ORC (organic Rankine cycle) has been investigated widely. ORC can be driven by low temperature hest source with the temperature of lower than 300 °C. ORC is favorable compared with conventional water-vapor Rankine cycle. The heat source of ORC can be solar energy, biomass energy, biogas energy, geothermal and industrial waste heat etc. ORC can also be driven by the waste heat in the cement industry to generate power or electricity. At present, the ORC investigations have been focused on the selection of working fluids, the cycle performance, the economy analysis and the environmental impact analysis.

The ORC performance is strongly dependent on the organic fluids. Lakew & Bolland [4] investigated ORCs using the fluids of R134a, R123, R227ea, R245fa, R290 and n-pentane. The results showed that the ORC with the fluid of R227ea yielded the maximum power output when the heat source temperatures were in the range of 80–160 °C. Meanwhile, R245fa produced highest power output with the heat source temperature in the range of 160–200 °C. Hung et al. [5] selected organic fluids by setting the system thermal efficiency as the target parameter. The turbine inlet pressure and temperature, turbine exit quality, condenser exit temperature, overall irreversibility and system efficiency were considered. The studies showed that wet organic fluids produced higher thermal efficiencies than dry fluids. A higher turbine inlet temperature and a lower condensation temperature could generate an economic feasible and environment friendly energy conversion system. Tchanche et al. [6] compared ORC efficiencies, volume flow rate,

* Corresponding author. Tel./fax: +86 10 61772163.
E-mail address: xjl@ncepu.edu.cn (J. Xu).

http://dx.doi.org/10.1016/j.energy.2015.03.112
0360-5442/

mass flow rate, pressure ratio, toxicity, flammability, ODP (ozone depletion potential) and GWP (global warming potential) using twenty organic fluids. It was found that R134 was more suitable for small scale solar energy utilizations. The fluids of R152a, R600a and R290 were attractive in the ORC thermal efficiencies. But attention should be paid to the flammability and safety issues of these fluids.

The frequently used ORC evaluation parameters were the thermal efficiency, heat recovery efficiency, exergy efficiency, net power or work, volume flow rate, expansion ratio in turbines, APR (heat exchanger area per unit power output), etc. Dai et al. [7] examined effects of various thermodynamic parameters on the ORC performance. They set the exergy efficiency as the objective parameter. ORCs were investigated using different working fluids under similar heat source conditions. It was found that ORCs were much better in their performances compared with water-vapor Rankine cycles. ORC with R236ea as the working fluid had maximum exergy efficiency. Roy et al. [8] investigated ORCs by setting the system thermal efficiency, turbine work output, irreversibility rate and second law efficiency as the objective parameters. The fluids of R123 and R134a were considered. They concluded that R123 had better ORC performance than R134 for low temperature waste heat utilizations. Wei et al. [9] optimized ORC using HFC-245fa as the working fluid. The increases in the work output and thermal efficiencies could raise the waste heat utilization degree. The running parameters of ORCs shall consider the environment impact. Roy et al. [10] maximized the work output and thermal efficiencies to optimize the turbine inlet pressure. The fluids of R12, R124, R134a and R123 were used, with R123 having the maximum work output and thermal efficiencies. Zhang et al. [11] used the thermal efficiency, exergy efficiency, recovery efficiency, APR and LEC (levelized energy cost) as the objective parameters to quantify the subcritical and transcritical ORCs for geothermal energy utilizations.

Recently, some researchers investigated the ORC environment impact and economic feasibility. Liu et al. [12] applied the LCA (life cycle assessment) to evaluate the EI (environment impact) for waste heat driven ORCs. It was found that the GWP (global warming potential) is the most serious EI followed by the HTP (human toxicity potential). Walsh & Thornley [13] evaluated the environment impact and economic feasibility for the metallurgical coke production process by introducing ORC to recover the waste heat in the process. It was found that introducing ORC to the coke generation process could reduce 1–3% of CO_2 emission, which was equivalent to decrease 10,000 tons of CO_2 emission annually. The discounted payback period was about three to six years. Tchanche et al. [14] investigated the economic feasibility of ORC for waste heat recovery. For a 2 kWe ORC, the specific installation cost was 5775 €/kW with a LEC (levelized electricity cost) of 13.27 c€/kWh. Alternatively, a 50 kWe ORC had the specific installation cost of about 3034 €/kW with the LEC of 7 c€/kWh. Kosmadakis et al. [15] reported the economic evaluation of two-stage solar driven ORC for reverse osmosis desalination. The specific fresh water cost was 6.85 €/m^3, approaching the value of the Photovoltaic-Reverse Osmosis system.

Here we investigate ORCs for waste heat recovery in the cement industry. Various organic fluids with proper thermodynamic parameters were considered. The technology-economy indicators of the NPV (net present value) and the PBP (payback period) were applied to evaluate the economic feasibility. Using the LCA data for China energy production, the ORC introduced to the cement production process was evaluated with one ton cement production as the functional unit.

2. The cement production process

Calcination is the core technique during the cement production process. The cement industry has experienced following stages in the history: the shaft kiln, dry hollow kiln, wet process kiln, lepol kiln, preheater kiln and outside pre-decomposition calciner. The NSP (New Suspension Preheater) cement production technology (including the suspension preheating and pre-decomposition technologies) becomes the main technology in the world due to its outstanding advantages for cement production. The NSP cement production process mainly include raw material mining and homogenizing, energy-saving grinding, high efficiency and low pressure drop pre-heater and calciner, grate cooler and high performance thermal insulation material.

The NSP cement production technique consisted of three main stages: raw material preparation, clinker sintering, cement production and storage. Fig. 1 shows the flow chart of the cement production process.

The raw material preparation stage treats the limestone and auxiliary raw material to satisfy the material sintering requirement, physically. The calcareous raw material, clayey raw material and ferro-controlling raw material are crushed and dried. Then they are sent to the material storage room where they are mixed according to specific ratios. The mixture is further milled to form high quality raw material powder, which is to be further homogenized.

The clinker sintering is one of the major processes for the NSP cement production, consisting of the outside-kiln preheating and decomposition, inside-kiln sintering, clinker cooling and exhausts gas processes. The raw material powder is elevated to the preheater where it is heated. The raw material receives heat from the hot gas stream in multi-pre-heaters to reach a high temperature. Then it enters the decomposition furnace to make the powders decomposition. The decomposed material is calcined to reach the partial melting state in the rotary kiln to form the high temperature clinker, which is then crushed and cooled in the kilneye.

The final cement production process is described as follows. The gypsum and slag are mixed with the clinker. The formed mixture is grinded into fine powders by the cement grinding machine. Then the cement is ready to be dispatched. The cement milling system and packaging system are involved in the final production process [16].

Usually, the NSP cement production line has the thermal utilization efficiency of about 50–60%. Table 1 shows the heat consumption percentage of various components or processes for a 4000 t/d cement production line of China. Except the heat consumed by the clinker, the pre-heater and the exhaust gas at the cooler outlet dissipated about 33% of the total heat. The outlet temperature of the kiln tail pre-heater is normally 330 °C. The exhaust gas at the kiln cooler outlet is 220 °C. Different cement production quantities have different waste heat quantities. This paper discussed the waste heat driven ORCs. The waste heat resource comes from the heat carrier fluid at the kiln cooler outlet. The main parameters can be found in Ref. [17]. The heat carrier fluid is hot air having its temperature of 220 °C and mass flow rate of 43.02–82.73 kg/s.

3. The ORC working principle

Fig. 2 shows a basic ORC configuration, mainly consisting of an expander, a condenser, a fluid circulating pump and an evaporator. Fig. 3 shows the T-s diagram. The thermodynamic cycle includes an expansion process (1–2), a condensation process (2–4), a pumping process (4–5) and an evaporation process (5–1). The following assumptions are made to simplify the analysis:

- The steady flow and heat transfer state within the ORC;
- The saturated liquid state at the condenser outlet;
- The saturated vapor state at the evaporator outlet;
- No heat loss from the ORC component to the environment;
- No pressure drops with fluid flowing in pipelines.

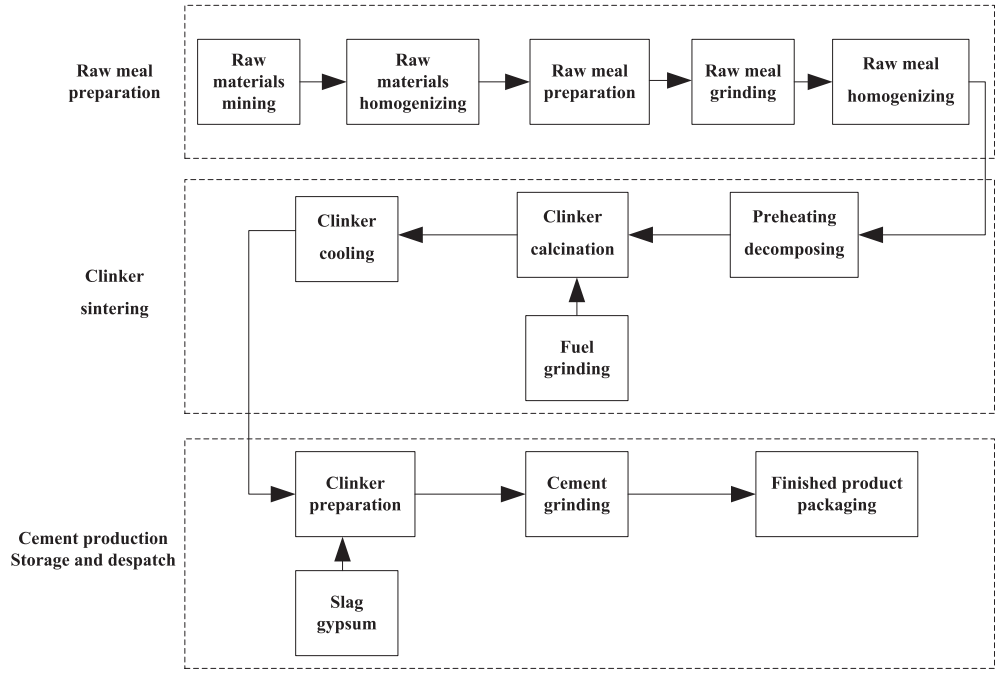

Fig. 1. The flow chart of the cement production line.

Table 1
The heat consumption for China 4000 t/d cement production line.

Item	Percentage	Item	Percentage
Heat required for clinker sintering	54%	Waste heat at the pre-heater outlet	22%
Waste heat at the cooler outlet	11%	Heat loss at the system surface	5.5%
Heat carried by the clinker from the cooler	2%	Heat required by hot air to dry coal	1.5%
Heat required by raw material drying	1.5%	Heat carried fly ash at the pre-heater outlet	0.8%
Heat loss due to incomplete combustion	0.5%	Heat carried by fly ash at the cooler outlet	0.08%
Other heat loss	1.12%	Total	100%

The expansion process (1–2): Vapor is expanding in the expander to generate power or work. An ideal assumption is the isentropic expansion. A practical entropy-increase expansion can be reflected by an isentropic efficiency η_s. The expansion power is written as

$$\dot{W}_t = \dot{m}_{wf}(h_1 - h_2) = \dot{m}_{wf}(h_1 - h_{2s})\eta_s \tag{1}$$

The condensation process (2–4): The superheated or saturated vapor is condensed to the saturated liquid in the condenser. The condensation heat is

$$\dot{Q}_{cond} = \dot{m}_{wf}(h_2 - h_4) = \dot{m}_{air}(h_{air,out} - h_{air,in}) \tag{2}$$

The pumping process (4–5): The organic liquid is circulated by a pump. The isentropic pumping is an ideal case. The practical pumping is an entropy-increase process which is considered by a pumping isentropic efficiency. The pumping power is written as

$$\dot{W}_p = \dot{m}_{wf}(h_5 - h_4) = \frac{\dot{m}_{wf}(h_{5s} - h_4)}{\eta_p} \tag{3}$$

The evaporation process (5–1): The organic liquid receives heat from the waste heat to form the saturated vapor at the evaporator outlet. The heat received from the heat source is

$$\dot{Q}_{ev} = \dot{m}_{wf}(h_1 - h_5) = \dot{m}_{wh}(h_{wh,in} - h_{wh,out}) \tag{4}$$

Thus, the net power generated by the ORC is

$$\dot{W}_{net} = \dot{W}_t - \dot{W}_p \tag{5}$$

The ORC thermal efficiency is

$$\eta_t = \frac{\dot{W}_{net}}{\dot{Q}_{ev}} \tag{6}$$

The waste heat recovery degree is the heat received from the waste heat divided by the waste heat directly released to the environment. The global thermal efficiency is the waste heat recovery degree multiplied by the ORC thermal efficiency [14]:

$$\varepsilon_r = \frac{\dot{Q}_{ev}}{\dot{Q}_{ev,\max}} = \frac{\dot{m}_{wh}c_{p,wh}(T_{wh,in} - T_{wh,out})}{\dot{m}_{wh}c_{p,wh}(T_{wh,in} - T_{amb})} = \frac{T_{wh,in} - T_{wh,out}}{T_{wh,in} - T_{amb}} \tag{7}$$

$$\eta_{global} = \varepsilon_r \eta_t \tag{8}$$

The pinch temperature difference quantifies the minimum temperature difference between the heat carrier fluid of the waste heat and the organic fluid, which is written as

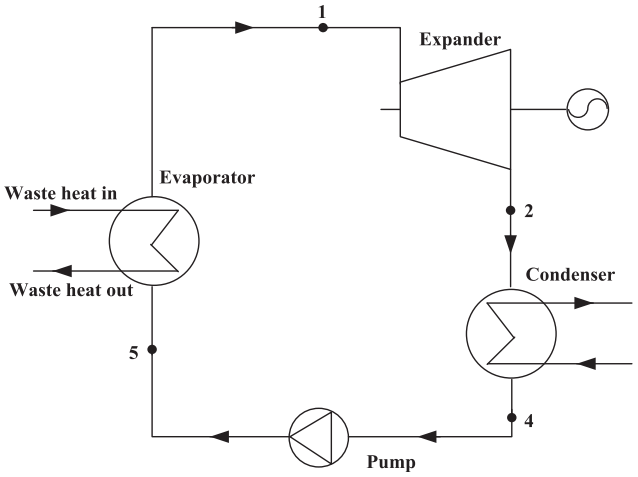

Fig. 2. The basic ORC configuration.

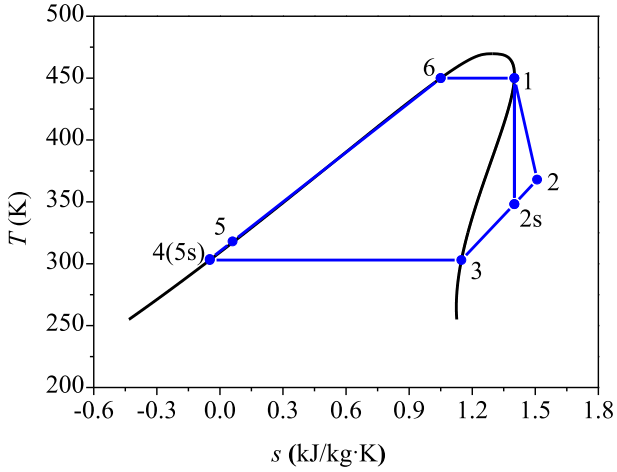

Fig. 3. The *T-s* diagram of organic Rankine cycle.

$$\Delta T_p = \frac{\dot{Q}_{ev} - \dot{Q}_{evtw}}{\dot{m}_{wh} C_{p,wh}} + T_{wh,out} - T_{ev} \tag{9}$$

where $\dot{Q}_{evtw}$ is the heat received from the heat source in the two-phase region, T_{ev} is the evaporation temperature, $C_{p,wh}$ is the specific heat of the heat carrier fluid of the heat source in terms of the temperature of $0.5(T_{wh,in} + T_{wh,out})$. The pinch temperature difference $\triangle T_p$ is a function of T_{ev}. Each T_{ev} has a specific $\triangle T_p$. The heat transfer process requires a positive $\triangle T_p$.

ORC uses the shell-tube heat exchangers. The air-side heat transfer coefficients for the evaporator and condenser are set to 70 W/m^2·K and 50 W/m^2·K, respectively [12]. The pinch temperature difference for the condenser is 5 K. Both the evaporator and condenser contain the single-phase liquid flow region and two-phase flow region. The heat transfer surface areas are based on Ref. [18].

The heat transfer area for the single-phase liquid region of the evaporator is

$$A_{ev,s} = \frac{\dot{Q}_{evs}}{K_e \Delta T_{evs}} = \frac{\dot{Q}_{ev} - \dot{Q}_{evtw}}{K_e \Delta T_{evs}} \tag{10}$$

where the temperature difference ΔT_{evs} is

$$\Delta T_{evs} = \frac{\Delta T_{evs,\max} - \Delta T_{evs,\min}}{\ln \frac{\Delta T_{evs,\max}}{\Delta T_{evs,\min}}} = \frac{T_{wh,out} - T_5 - \Delta T_p}{\ln \frac{T_{wh,out} - T_5}{\Delta T_p}}$$

The heat transfer area for the two-phase region of the evaporator is

$$A_{ev,tw} = \frac{\dot{Q}_{evtw}}{K_e \Delta T_{evtw}} \tag{11}$$

where $\Delta T_{evtw} = \frac{T_{wh,in} - T_1 - \Delta T_p}{\ln \frac{T_{wh,in} - T_1}{\Delta T_p}}$

Thus the evaporator has the following heat transfer area:

$$A_{ev} = A_{ev,s} + A_{ev,tw} \tag{12}$$

The condenser has the heat transfer area of the single-phase liquid region of

$$A_{cond,s} = \frac{\dot{Q}_{conds}}{K_{cond} \Delta T_{conds}} \tag{13}$$

where $\Delta T_{conds} = \frac{T_2 - T_{air,out} - \Delta T_{cond}}{\ln \frac{T_2 - T_{air,out}}{\Delta T_{cond}}}$.

The condenser has the heat transfer area of the two-phase region of

$$A_{cond,tw} = \frac{\dot{Q}_{condtw}}{K_{cond} \Delta T_{condtw}} \tag{14}$$

where $\Delta T_{condtw} = \frac{T_4 - T_{air,in} - \Delta T_{cond}}{\ln \frac{T_4 - T_{air,in}}{\Delta T_{cond}}}$.

The condenser has the following total heat transfer area

$$A_{cond} = A_{cond,s} + A_{cond,tw} \tag{15}$$

The total heat transfer area of the evaporator and condenser is

$$A_{tot} = A_{ev} + A_{cond} \tag{16}$$

4. Results and discussion

4.1. Verification of the ORC thermodynamic analysis

In order to compare the computation results with the experimental data, an ORC was built in the authors' laboratory (see Fig. 4a). Major components were marked as conduction oil boiler, electric valve, piston pump, condenser, data acquisition system, expander, torque and speed sensor and dynamometer. Fig. 4b shows the scroll expander and dynamometer. Fig. 4c shows the expander. Fig. 4d–e shows the rotating scroll and fixed scroll of the expander, respectively.

Four subsystems were coupled with each other. The ORC loop mainly consisted of a piston pump, an evaporator, an expander and a condenser. The piston pump circulated the R123 fluid. The pump was controlled by a frequency converter to regulate R123 flow rate. The evaporator was a tube-in-tube heat exchanger, having a heat transfer area of 5.53 m^2. The expander was modified from a scroll compressor for the bus-used air-conditioning system. Because the compressor had simple structure and high reliability and it was available commercially, it was considered as one of the promising candidates for the expander in kW-scale capacity. Some modifications were performed so that it was suitable to work as an expander. The designed shaft power of the expander was about 4 kW. The condenser was a plate heat exchanger with a heat transfer area of 6.08 m^2.

An *AC* dynamometer dynamically measured the rotating speed (n_{exp}), shaft torque (M_{exp}) and power (W_{exp}) of the expander. The unit consisted of a frequency converter, an *AC* motor, a rotating speed sensor, a monitor, a software and transmission facilities. The power was transmitted by a belt and couplings to the *AC* motor. The

rated rotating speed and the maximum shaft torque of the *AC* motor were 1495 rpm and 70.26 N m, respectively. The computer software dynamically processed the rotating speed and shaft torque of the expander with the help of sensors. The software communicated with the frequency converter to control the shaft torque of the *AC* motor. During the system operating, the shaft torque of the *AC* motor was set by the software to be a specific percentage of the maximum value (70.26 N m here). The frequency converter of the *AC* motor controlled the shaft torque to maintain the desired value. In such a way, the shaft power of the expander was directly measured.

The conductive oil was heated by an electric heater with a 100 kW capacity. The electric heater automatically adjusted the heating power to satisfy the required oil temperature, having the maximum value of 300 °C. The temperature could be controlled with an uncertainty of 1 °C. An oil pump circulated the conductive oil which received heat from the electric heater and dissipated heat to the ORC evaporator. The oil mass flow rate was measured by a mass-flow-meter. The oil temperature entering and leaving the ORC evaporator were to evaluate the total heat dissipated to ORC.

The expander operation needed lubricant, which was circulated by a gear pump. The lubricant was mixed with the R123 vapor at the expander inlet. After the expansion, the lubricant was separated from the R123 vapor by an efficient vapor-oil separator. Then, the lubricant returned to the oil tank.

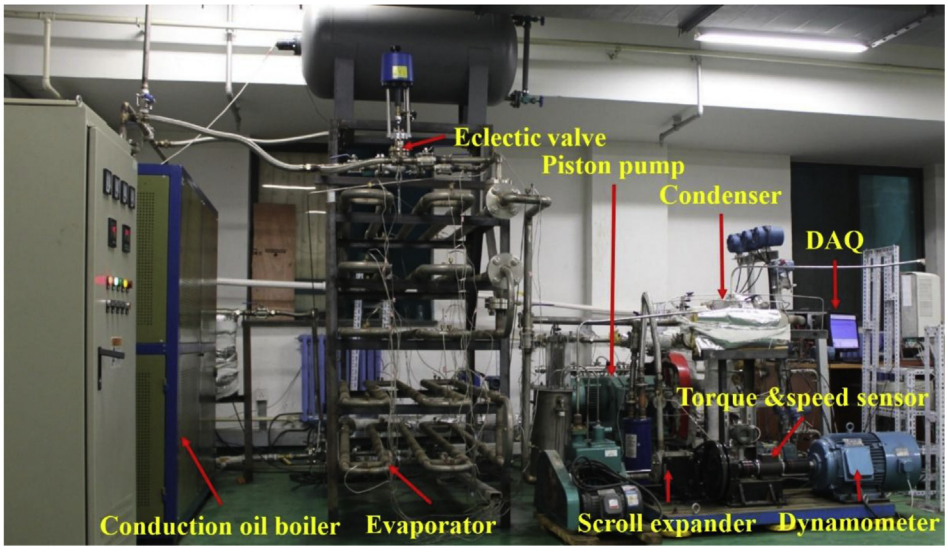

(a)

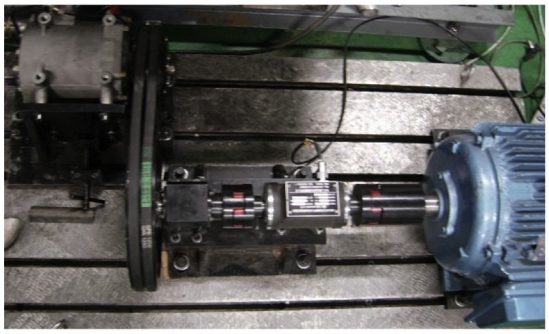

(b)

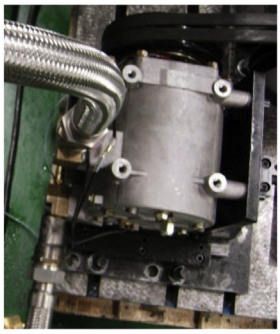

(c)

(d)

(e)

Fig. 4. The ORC photo: (a) ORC system; (b) fixed scroll expander and dynamometer; (c) expander; (d) rotating scroll; and (e) fixed scroll.

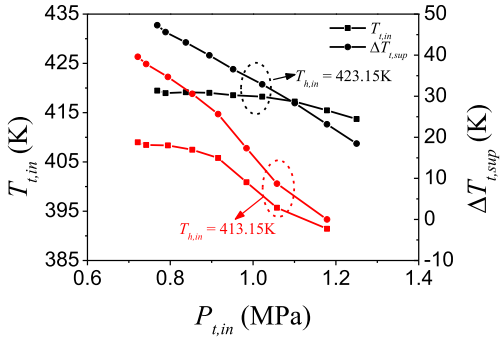

Fig. 5. The measured expander inlet temperature, vapor superheating versus expander inlet pressure.

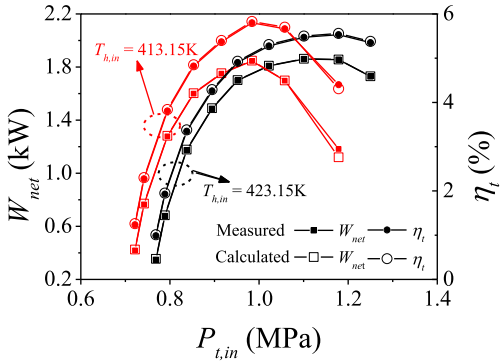

Fig. 6. The measured expander powers and system thermal efficiencies versus expander inlet pressures compared with the computed values.

The cooling water loop was thermally coupled with the ORC condenser. It dissipated extra heat of ORC to the air environment. The outdoor spray cooling tower was the key component of the cooling water loop. The tower had the cooling capacity of about 73 kW, corresponding to the water flow rate of 5000 kg/h, at which the temperature difference of the cooling water loop was 12.5 °C. Mass flow rate and temperatures were measured to monitor the operation of the cooling water loop.

The measured conductive oil temperature entering the ORC evaporator was 423.15 K and 413.15 K, respectively. Fig. 5 shows the measured expander inlet temperature and vapor superheating versus expander inlet pressures. The isentropic efficiencies of the organic fluid pump and expander were in the range of 16.88–29.91% and 24.03–64.88%, respectively. Fig. 6 shows the measured expander powers and system thermal efficiencies versus expander inlet pressures compared with the computed values. The computed data agreed with the measured data well, demonstrating the correctness of the ORC thermodynamic analysis coupled with the heat source.

Due to the wide applications of ORC in industries, various organic fluids were suggested in the literature. Wang et al. [19] investigated the effect of molecular structures and entropies on the ORC thermal efficiencies. A subcritical pressure ORC was considered with an evaporation temperature of 90 °C and a condensation temperature of 35 °C. They noted that the working fluids with low molecular entropies could generate high thermal efficiencies. Rayegan and Tao [20] identified the most suitable fluids to operate a solar energy driven ORC. The authors calculated the thermal efficiency with flexible evaporation temperatures. They found that higher critical temperatures of organic fluids allowed higher evaporation temperature to reach higher thermal efficiencies. The above conclusion was correct for specific evaporation temperatures such as 130 °C and 85 °C. Kosmadakis et al. [21] selected the "best" fluid for an ORC included in a two-stage combined system for RO (reverse osmosis) desalination application. The thermal efficiency of R245fa was acceptable and its use was not restricted by any international regulations, even though the thermal efficiency was not the highest. Mikielewicz and Mikielewicz [22] proposed the Jakob number criterion for fluid selection. Kuo et al. [23] investigated the effect of working fluids on ORC performance with an ORC power output in 50 kW capacities. A dimensionless "figure of merit" combining the Jakob number, evaporating temperature and condensing temperature was proposed as far as the thermal efficiency was concerned.

Recently, Xu and Yu [24] proposed the critical temperature criterion for fluid selection. The core concept is as follows. It is known that the ORC evaporator operates at the highest temperature level. The evaporator contributes the largest exergy destruction over the whole ORC components. Thus, improvement of the evaporator can apparently increases the ORC thermal efficiency. An integration temperature difference was defined as follows:

$$\Delta T_i = \frac{\int_0^{Q_t} (T_{hot} - T_{cold}) dQ}{Q_t} \tag{17}$$

where the numerator of Eq. (17) represents the enclosed area of the T-Q (or ΔH) curves of the hot and cold fluids, Q_t is the total heat transfer rate, T_{hot} and T_{cold} are the hot and cold fluid temperatures, respectively. It is noted that ΔT_i is a process parameter, depending on the heat transfer path. Xu and Yu [24] shows that ΔT_i has a linear relationship with the evaporator exergy destruction. The decrease of ΔT_i increases the ORC thermal efficiency.

It is shown that the critical temperature can be the sole criterion for the fluid selection. The increase of critical temperature decreases the integration temperature difference of the evaporator. Thus, the exergy destruction of the evaporator is decreased to increase the ORC thermal efficiency. When the critical temperature approaches or is beyond the hot source temperature, the ORC thermal efficiency is only slightly decreased. Thermal efficiencies had scattered distribution versus any other parameters except the critical temperatures.

Five organic fluids were used here: R245fa, R123, R601, isohexane and hexane, with critical temperatures (T_c) from low to high (Table 2). Fig. 7 shows that the ORC thermal efficiencies are

Table 2
The major parameters of the five working fluids.

Working fluid	Formula	T_c (K)	P_c (MPa)	Toxicity	Flammability	ODP	GWP_{100}
Hexane	C_6H_{14}	507.82	3.03	2.094	Highly	0	–
Isohexane	C_6H_{14}	497.7	3.04	Low	Highly	0	–
R601	C_5H_{12}	469.7	3.37	Low	Extremely	0	11
R123	$C_2HCl_2F_3$	456.83	3.66	High	None	0.012	120
R245fa	$C_3H_3F_5$	427.16	3.65	None	None	0	820

Note: T_c is the critical temperature, P_c is the critical pressure, ODP represents ozone depletion potential and GWP represents global warming potential.

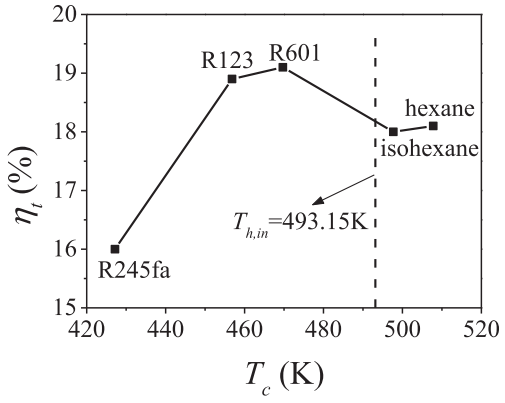

Fig. 7. The ORC thermal efficiencies versus the fluid critical temperatures.

increased with critical temperatures. The R601 held the maximum thermal efficiency, due to its critical temperature approaching the hot source temperature of 493.15 K. The fluids of isohexane and hexane slightly weaken the thermal efficiencies, due to their critical temperatures being larger than the hot source temperature of 493.15 K Fig. 8 explains the trend of thermal efficiencies against critical temperatures. The enclosed areas of hot and cold fluid are gradually decreased from R245fa to R601. The enclosed area for R601 was the smallest. When the critical temperature is larger than the heat source temperature such as shown in Fig. 8d–e, the red (in web version) envelop curve of the fluid crossed the *T*-*Q* curve of the hot fluid. The enclosed area of hot and cold fluid is slightly increased to slightly worsen the thermal efficiencies.

4.2. The ORC computation

In this study, the waste heat for ORC is the dry air at the kiln cooler outlet. The NSP China cement production line is selected. The line has the production rates of 4000 tons per day and 1.24 million tons per year. The kiln has the operating ratio of about 85% each year. The heat carrier fluid of dry air enters the ORC evaporator at 220 °C and leaves the ORC evaporator at 90 °C. The dry air has the mass flow rate of 43.01 kg/s. The isentropic efficiencies of the expander and pump are 85% and 80%, respectively. The organic vapor is condensed in the condenser by the environmental air with the temperature of 293.15 K. The organic fluid reaches the saturation temperature of 303.15 K after leaving the condenser.

Fig. 9 shows the ORC thermal efficiency, the global thermal efficiency and the pinch temperature difference in the evaporator versus the evaporation temperature. Fig. 9a shows that the ORC increased its thermal efficiencies and global thermal efficiencies

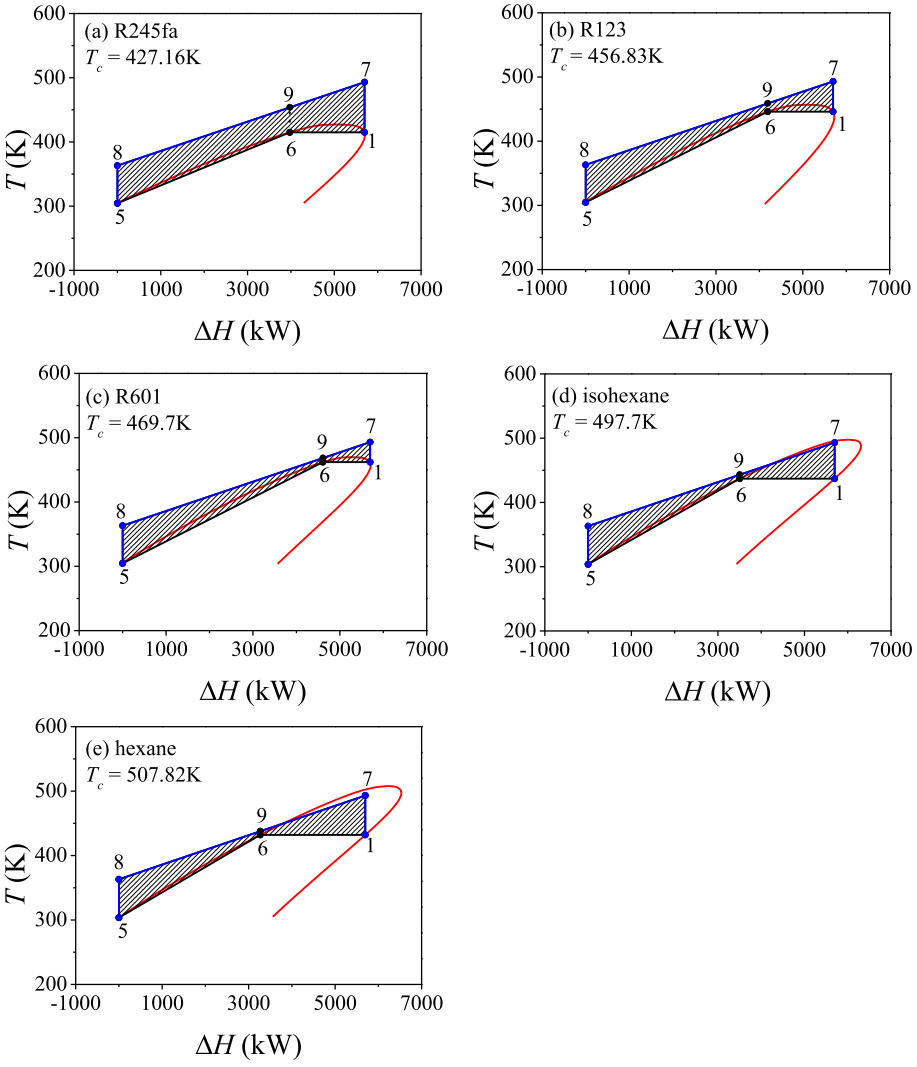

Fig. 8. The *T*-*Q* curves for the five organic fluids.

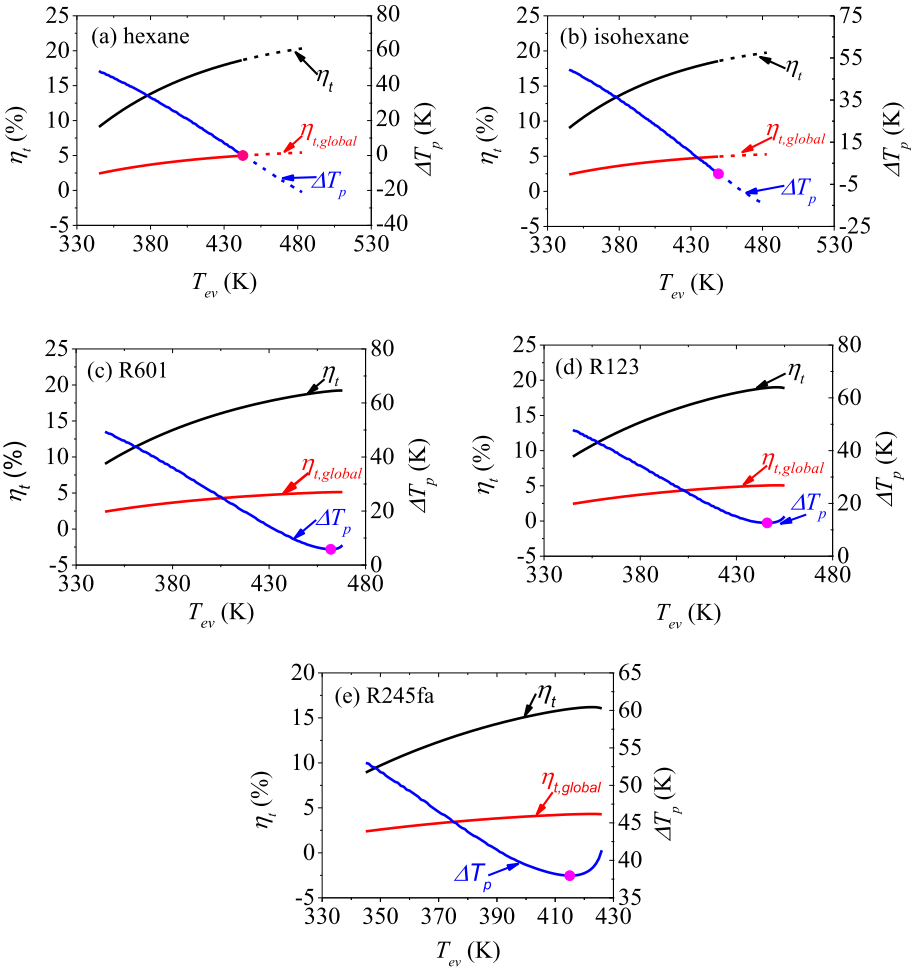

Fig. 9. The thermal efficiency, global thermal efficiency and pinch point temperature versus the evaporation temperature.

with increases in the evaporation temperatures for hexane. The maximum η_t and $\eta_{t,global}$ are 18.7% and 4.99%, respectively when T_{ev} was 442.8 K at which $\triangle T_p$ was 0 K. Further increases in the evaporation temperatures yield negative pinch temperature difference, which is not practical for real heat transfer process. The solid pink (in web version) point represents the state at which $\triangle T_p = 0$ K. Similarly, Fig. 9b shows that ORC reached maximum thermal efficiency η_t of 18.5% and global thermal efficiency $\eta_{t,global}$ of 4.95%, respectively, corresponding to T_{ev} of 449.2 K at $\triangle T_p = 0$ K (the pink point). Fig. 9c–e shows somewhat different trend of those in Fig. 9a–b. With continuous increases in the evaporation temperatures, the pinch temperature differences are reduced to the minimum point and then increased, which are always positive. The ORC thermal efficiencies and global thermal efficiencies are increased versus T_{ev} and reach the maximum values of 19.1% and 5.1% for R601 in Fig. 9c and 18.9% and 5.1% for R123 in Fig. 9d, and 16% and 4.3% for R245fa in Fig. 9e. These maximum efficiencies happen at the minimum pinch temperature differences.

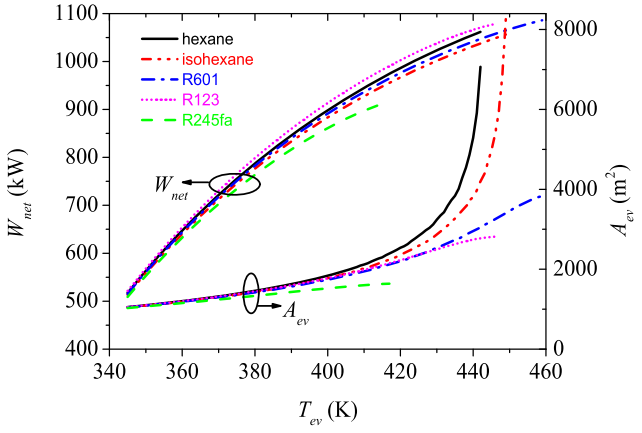

Fig. 10. The power output and evaporator surface area versus the evaporation temperature at the mass flow rate of hot air of 43.02 kg/s.

The ORC thermal performance is determined by the thermal efficiency, pinch temperature difference and evaporation temperature. Fig. 10 shows the increased net power output and heat transfer surface area with increases in the evaporation temperatures. Table 3 gave the ORC performance parameters for the five working fluids, in which R601 had the maximum net power output and thermal efficiency. This trend can be explained by the critical temperature of R601 approaching the heat source temperature.

4.3. Economic analysis

The NPV (net present value) method is efficient to evaluate the ORC economic performance. The NPV is the difference between the net cash flow generated by the investment for the capital cost

Table 3
The ORC parameters using five organic fluids.

Working fluids	T_{ev} (K)	$\triangle T_p$ (K)	η_t (%)	$\eta_{t,global}$ (%)	W_{net} (kW)	W_p (kW)	A_{ev} (km^2)	A_c (km^2)	A (km^2)
Hexane	432	6.33	18.1	4.83	1029.91	16.30	3.426	10.778	14.204
Isohexane	437	6.39	18.0	4.79	1023.21	21.85	3.473	10.529	14.002
R601	462	5.82	19.1	5.11	1090.74	58.84	3.867	10.943	14.810
R123	446	12.60	18.9	5.05	1078.16	63.34	2.815	12.280	15.095
R245fa	415	37.95	16.0	4.30	911.30	59.77	1.630	12.737	14.367

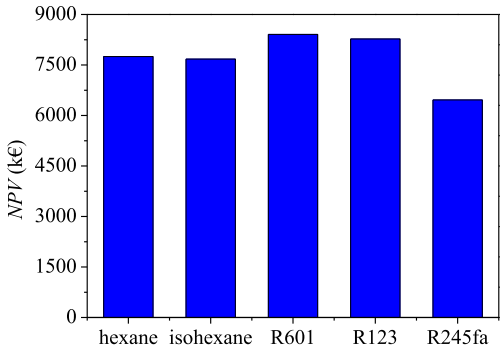

Fig. 11. The NPV of ORC.

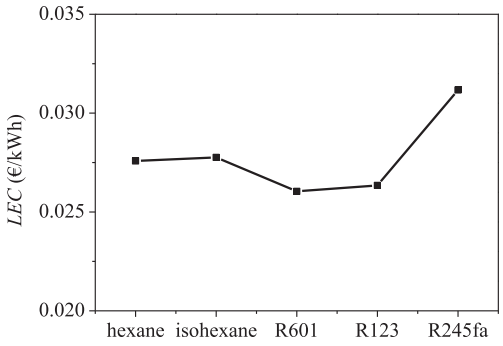

Fig. 13. The LEC of ORC.

discount and the present value of the initial investment cost. The NPV is calculated as [14]:

$$NPV = -C_0 + \sum_{n=1}^{N} \frac{F_n}{(1+k)^n} \tag{18}$$

where $_N$ is the life cycle time, F_n is the net cash flow for the fiscal year n: F_n=B_n–C_n, B_n is the benefit (inflows) for the fiscal year n, C_n is the cost (outflows) for the fiscal year n, C_0 is the initial investment, k is the interest rate.

The evaluation criterion is that the investment is feasible for NPV $\geq$ 0 and infeasible for NPV < 0. The optimal strategy exists for the maximum net cash flow. The NPV method considers the capital time value and the net cash flow of the entire process to enhance the investment economic evaluation. The NPV method reflects the balance between the fluidity and profitability. Thus, the method expresses the investment risk. The high risk investment is recommended to use high discount rate. One the contrary, the low risk investment uses the low discount rate.

However, the investment plan is difficult to be evaluated by the NPV method if the investment cost is not clear. Under such circumstance, the PBP (payback period) can evaluate the investment plan. The PBP is the time on which the initial investment is recovered. The PBP is the value of N when NPV equals to zero. Assuming the constant F_n, the following equation exists based on Eq. (18).

$$PBP = -\ln(1 - kC_0/F_n)/\ln(1+k) \tag{19}$$

The ORC investment costs include the expander, evaporator, condenser, pump, organic fluid, pipeline, control system, auxiliary equipments and labor cost. The net power output generated by ORC is fixed to be 1 MW based on Fig. 10. The investment cost data comes from Ref. [13]. The total cost was 2115 k€ corresponding to the specific cost of 2.115 k€/kW. The system maintenance and consumptive material cover 2% and 0.3% of the total costs, respectively. The management and insurance cover 0.7% of the total costs.

The ORC system is assumed to have the lifetime of 20 years, the load factor of 85% and the system degradation rate of 2%, with the interest rate of 5%. The industry electricity price is 1 ¥/kWh, equivalent to 0.117 €/kWh according to the money exchange rate on April 2, 2014. The comprehensive energy consumption for the

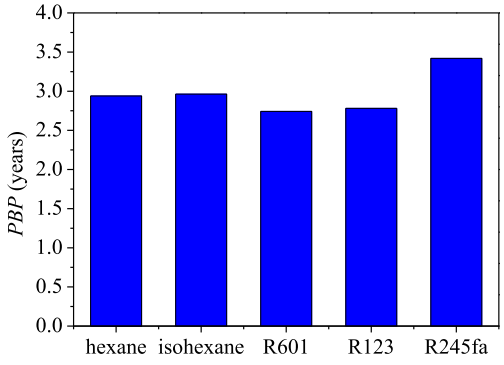

Fig. 12. The PBP of ORC.

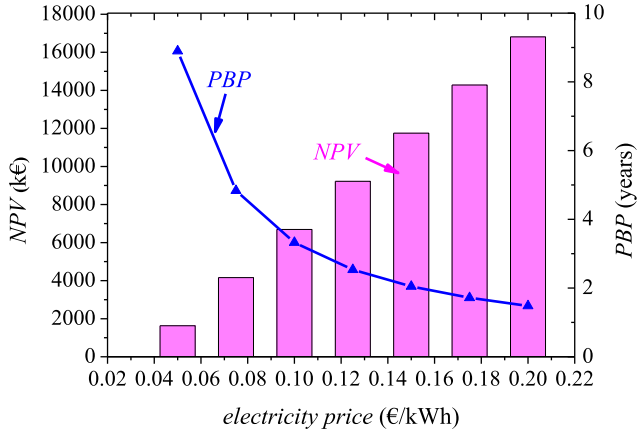

Fig. 14. The NPV and PBP changed with the electricity price.

Table 4
The annual gas emission reduction by integrating ORC for the 4000 t/d cement production line.

Working fluids	Emissions	CO_2	SO_2	NO_x	CO
Hexane	Quantity (t)	8751.5	79.1	40.0	21.3
Isohexane	Quantity (t)	8694.6	78.6	39.7	21.1
R601	Quantity (t)	9268.4	83.8	42.4	22.5
R123	Quantity (t)	9161.5	82.8	41.9	22.3
R245fa	Quantity (t)	7743.7	70.0	35.4	18.8

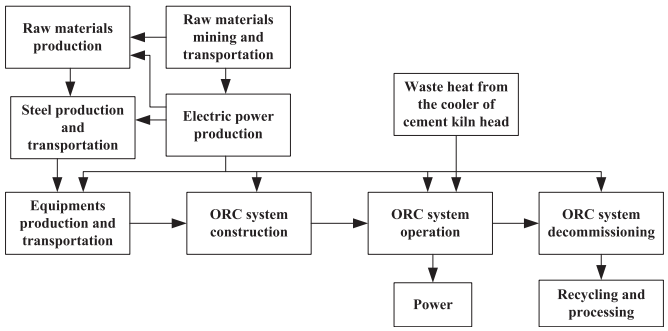

Fig. 15. The boundary of ORC.

4000 tons/day cement production line is about 100 kWh/ton. The annual energy consumption is 134 MkWh for the cement production line. The ORC generated electricity with the organic fluids of hexane, isohexane, R601, R123 and R245fa is 76,68,710 kWh, 76,18,822 kWh, 81,21,650 kWh, 80,27,979 kWh and 67,85,540 kWh per year, equivalent to save 2300 tons, 2285 tons, 2436 tons, 2408 tons and 2035 tons standard coal, respectively. If the generated electricity is self consumed by the cement production line, it can save the electric charge of 897.2 k€, 891.4 k€, 950.2 k€, 939.2 k€ and 793.9 k€, respectively. Fig. 11 shows the NPV values, which are 7748.7 k€, 7676.0 k€, 8409.1 k€, 8275.5 k€ and 6461.0 k€ for the five working fluids. Fig. 12 shows the PBP values, which are 2.94, 2.96, 2.74, 2.78 and 3.42 years, respectively. Fig. 13 shows the LEC values, which is 2.758 c€/kWh, 2.776 c€/kWh, 2.604 c€/kWh, 2.635 c€/kWh and 3.117 c€/kWh, respectively. It can see that the NPV, PBP and LEC values of the ORC system have the consistent change trends to those of the ORC net power output and thermal efficiencies, with respect to the working fluids. The ORC with the fluid of R601 had the maximum NPV and minimum PBP and LEC. On the contrary, the ORC with the fluid of R245fa had the minimum NPV and maximum PBP and LEC values. This is because R601 has the critical temperature approaching the heat source temperature of 220 °C. Based on our studies in Refs. [24], the ORC with R601 as the working fluid had better thermal performance. It is noted that the NPV and PBP values are influenced by the electricity price (see Fig. 14). When the electricity price is increased, the NPV values are increased but the PBP values are decreased, for the ORC with the fluid of R601.

4.4. Environmental assessments

4.4.1. Evaluation of direct emission reduction

The ORC integrated with the cement production line generates high grade electricity to decrease the electricity consumption and reduce the gas emission. The LCA (life cycle assessment) shows that the 4000 t/d cement production line discharges 12,51,454 tons CO_2, 1823 tons SO_2, 2602 tons NO_x and 386 tons CO per year [25]. Table 4 shows the data of the gas emission. The reduced emission ratio is defined as the reduced gas emission integrated with ORCs divided by the gas emission without ORC involved. The gas reduction emission ratios are insensitive to the working fluids used. For the organic fluids with critical temperatures from high to low, the reduction ratios were 0.70%, 0.69%, 0.74%, 0.73% and 0.62% for CO_2, 4.33%, 4.30%, 4.59%, 4.53% and 3.83% for SO_2, 1.54%, 1.53%, 1.63%, 1.61% and 1.36% for NO_x, 5.51%, 5.47%, 5.83%, 5.77% and 4.87% for CO.

4.4.2. LCA (life cycle assessment)

In order to assess the environment impact of introducing ORC to the cement production line, the LCA method is applied obeying the ISO14040 standard. The LCA strategy includes four steps: definition of the goal and scope, the inventory analysis, the impact assessment and the LCA explanation. In this study, the function unit was selected to be one ton cement production.

In order to simplify the analysis, the cement production line and the ORC system were assessed by the LCA method, independently. Then, the environment impact of the combined system was achieved using the data of the two independent systems. The LCA data of the cement production line was cited from Ref. [25]. This paper majorly achieved the LCA data for the ORC system. ORC was evaluated regarding the environment impact from the cradle to grave. The stainless steel was the major material to fabricate ORC, neglecting other material consumption. Fig. 15 shows the boundaries of the ORC system, including the raw material milling, production and using, as well as the system construction, operation and decommissioning.

Because ORC recovers waste heat from the kiln cooler outlet, the ORC system uses the available room to be integrated with the cement production line. No additional building is needed for the ORC integration thus the building cost is negligible. The ORC construction stage mainly considers the raw material milling, production and transportation. During the ORC operation stage, the ORC self-generated electricity drives the fluid circulating pump. Thus, the ORC operation does not increase additional gas emission. The ORC decommissioning stage mainly treats the waste disposal and recycling. The ORC is made of the stainless steel, which should be recycled in this stage. The road transportation is the major factor to be considered for the ORC waste recycling. The transportation

Table 5
The increased gas emissions due to introduction of ORC for one ton cement production.

Emissions (kg/t)	Hexane	Isohexane	R601	R123	R245fa
CO_2	2.66×10^{-1}	2.62×10^{-1}	2.77×10^{-1}	2.82×10^{-1}	2.69×10^{-1}
NH_4	2.57×10^{-5}	2.54×10^{-5}	2.68×10^{-5}	2.74×10^{-5}	2.60×10^{-5}
NO_x	8.18×10^{-3}	8.07×10^{-3}	8.53×10^{-3}	8.70×10^{-3}	8.28×10^{-3}
CO	2.96×10^{-2}	2.92×10^{-2}	3.09×10^{-2}	3.15×10^{-2}	2.99×10^{-2}
HC	3.65×10^{-3}	3.60×10^{-3}	3.81×10^{-3}	3.88×10^{-3}	3.69×10^{-3}
SO_2	2.02×10^{-3}	1.99×10^{-3}	2.10×10^{-3}	2.14×10^{-3}	2.04×10^{-3}
H_2S	1.24×10^{-7}	1.23×10^{-7}	1.30×10^{-7}	1.32×10^{-7}	1.26×10^{-7}
HCl	1.25×10^{-6}	1.23×10^{-6}	1.30×10^{-6}	1.33×10^{-6}	1.26×10^{-6}
SW	6.95×10^{-3}	6.85×10^{-3}	7.25×10^{-3}	7.39×10^{-3}	7.03×10^{-3}
SA	4.29×10^{-4}	4.23×10^{-4}	4.47×10^{-4}	4.56×10^{-4}	4.34×10^{-4}

Table 6
Equivalency factor.

Type	Emissions	Equivalency factor
GWP	CO_2	1
	NH_4	25
	NO_x	320
	CO	2
AP	SO_2	1
	NO_x	0.7
	H_2S	1.88
	HCl	0.88
EP	NO_x	1.35
	NH_4	3.44
	NO_3	1
HTP	CO	0.012
	SO_2	1.2
	NO_x	0.78
SWP (solid waste potential)	Solid waste	1
SAP (soot and dust potential)	Soot and dust	1

distance is 186.72 km based on the 2012 statistics data [1]. In terms of Ref. [12], expander requires the stainless steel consumption of 1.2 kg for 1 kW power output. The thickness of the stainless steel for fabrication of heat exchangers is 6.35 mm.

The basic gas emission data were cited from the RCEES, CAS (Research Center for Eco-Environmental Sciences, Chinese Academy of Sciences) [26]. The production of 1 kg stainless steel discharges 410 g CO_2, 0.9 g NH_4, 0.8 g NO_x, 5.5 g CO, 0.095 g HC, 2.55 g SO_2, 0.00435 g H_2S, 0.0437 g HCl, 243 g SW (solid waste) and 1.5 g SA (soot and dust). The generation of 1 kWh electricity discharges 1141.2 g CO_2, 10.314 g SO_2, 5.2164 g NO_x, 2.772 g CO, 45.792 g SW and 9.5472 g SA in China. The one t·km truck transportation discharges 23.77 g CO_2, 2.758 g CO, 0.3416 g HC, 0.182 g SO_2 and 0.7641 g NO_x. Table 5 lists the finally obtained gas emission data for the ORC system.

Usually, the environment impact can be evaluated by ranking the gas emission data qualitatively or quantitatively. Here we used the model developed by RCEES, CAS. The model evaluates the contribution degree of the environment impact induced by the exchange between the studied system and the environment [26]. The model consists of following steps.

(1) The potential environment impact

$EP(j)$ is the contribution of the studied system on the jth potential environment impact:

$$EP(j) = \sum EP(j)_i = \sum \left[Q(j)_i \times EF(j)_i\right] \tag{20}$$

where $EP(j)_i$ is the contribution of the ith substance emission on the jth environment impact, Q_i is the ith substance emission quantity, $EF(j)_i$ is the equivalent factor of the ith substance emission on the jth potential environment impact. Table 6 lists the equivalent factor. Table 7 shows the potential environment impact data. The ORC with the fluid of isohexane generates smallest $EP(j)$. The potential environment impact is ranked from small to large for ORCs with the fluids of isohexane, hexane, R601, R123 and R245fa. The gas emission is mainly dependent on the stainless steel quantity for ORC construction. The ORC with the fluid of isohexane needs smallest heat exchanger surface area. On the contrary, the ORC with R123 needs largest heat transfer area to increase the potential environment impact.

(2) The data standardization

$$NP(j) = P(j)\frac{1}{TR(j)} \tag{21}$$

Table 7
The weighting potential of the environment impact due to introduction of ORC for one ton cement production.

Work fluids	Type	Environment potential (kg/t)	Standardize benchmarks (kg/(p.a))	Weighting factors	Weighting potential ($PE_{China,90}$)
Hexane	GWP	2.94	8700	0.83	2.81×10^{-4}
	AP	7.75×10^{-3}	36	0.73	1.57×10^{-4}
	EP	1.11×10^{-2}	62	0.73	1.31×10^{-4}
	HTP	9.16×10^{-3}	24.65	0.73	2.71×10^{-4}
	SWP	6.95×10^{-3}	251	0.62	1.72×10^{-5}
	SAP	4.29×10^{-4}	18	0.61	1.45×10^{-5}
Isohexane	GWP	2.90	8700	0.83	2.77×10^{-4}
	AP	7.64×10^{-3}	36	0.73	1.55×10^{-4}
	EP	1.10×10^{-2}	62	0.73	1.29×10^{-4}
	HTP	9.03×10^{-3}	24.65	0.73	2.67×10^{-4}
	SWP	6.85×10^{-3}	251	0.62	1.69×10^{-5}
	SAP	4.23×10^{-4}	18	0.61	1.43×10^{-5}
R601	GWP	3.07	8700	0.83	2.93×10^{-4}
	AP	8.08×10^{-3}	36	0.73	1.64×10^{-4}
	EP	1.16×10^{-2}	62	0.73	1.37×10^{-4}
	HTP	9.55×10^{-3}	24.65	0.73	2.83×10^{-4}
	SWP	7.25×10^{-3}	251	0.62	1.79×10^{-5}
	SAP	4.47×10^{-4}	18	0.61	1.52×10^{-5}
R123	GWP	3.13	8700	0.83	2.99×10^{-4}
	AP	8.23×10^{-3}	36	0.73	1.67×10^{-4}
	EP	1.18×10^{-2}	62	0.73	1.39×10^{-4}
	HTP	9.73×10^{-3}	24.65	0.73	2.88×10^{-4}
	SWP	7.39×10^{-3}	251	0.62	1.82×10^{-5}
	SAP	4.56×10^{-4}	18	0.61	1.55×10^{-5}
R245fa	GWP	2.98	8700	0.83	2.84×10^{-4}
	AP	7.83×10^{-3}	36	0.73	1.59×10^{-4}
	EP	1.13×10^{-2}	62	0.73	1.33×10^{-4}
	HTP	9.26×10^{-3}	24.65	0.73	2.74×10^{-4}
	SWP	7.03×10^{-3}	251	0.62	1.74×10^{-5}
	SAP	4.34×10^{-4}	18	0.61	1.478×10^{-5}

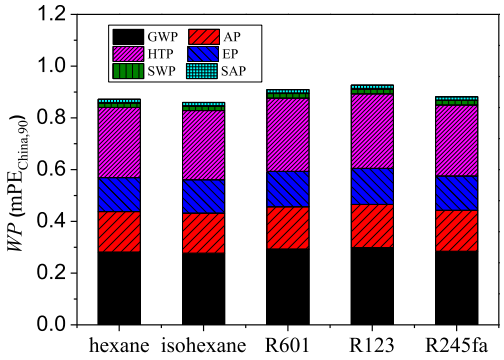

Fig. 16. The weighting potential.

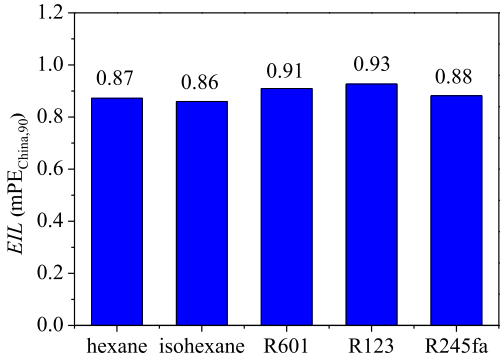

Fig. 17. Environment impact load.

where T is the product service duration, $R(j)$ is the benchmark data for the jth fiscal year, $P(j)$ is the potential environment impact or the resource consumption.

(3) The weighting of the potential environment impact

$$WP(j) = EP(j)/ER(j)_{T2000} \tag{22}$$

where $ER(j)_{T2000}$ is the sum of global or regional potential environment impact for the fiscal year of 2000.

(4) The EIL (environment impact load)

$$EIL = \sum WP(j) \tag{23}$$

In order to compare various environment impacts, the environment potentials were standardized and weighted to obtain GWP, AP (acidification potential), EP, HTP, SWP and SAP values (see Table 7). Fig. 16 shows the weighting potentials of environment impacts. The GWP effect covered 32.21%, which was the most serious, followed by the HTP effect having the ratio of 31.10%. The other impacts were ranked as AP (18.01%), EP (15.04%), SWP (1.97%) and SAP (1.67%). Fig. 17 shows the environment impact loads for ORCs using different organic fluids. The fluids that are used in ORCs were ranked as isohexane, hexane, R245fa, R601 and R123 to have the environment impact loads from low to high.

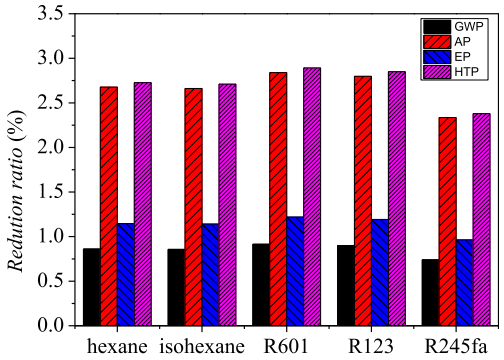

Fig. 18. The reduction ratio of weighting potential.

The gas emissions of CO_2, CO, NO_x and SO_2 were mainly considered during the cement production process. The weighting potentials of environment impact were GWP of 0.160 $PE_{China,90}$, AP of 0.060 $PE_{China,90}$, EP of 0.033 $PE_{China,90}$, and HTP of 0.101 $PE_{China,90}$. Obviously, *GWP* was the most serious. Table 8 shows the weighting potentials after introducing ORC to the cement production line. Fig. 18 shows the reduction ratios of weighting potentials. The ORC with R601 as the working fluid had minimum weighting potential and largest reduction ratios (GWP of 0.92%, AP of 2.84%, EP of 1.22% and HTP of 2.89%). On the contrary, the ORC with R245fa as the working fluid had smallest reduction ratios (GWP of 0.74%, AP of 2.34%, EP of 0.96% and HTP of 2.38%). The reduction ratio of weighting potential is related to the net ORC power output.

The ORC with the fluid of isohexane had the smallest environment potential when the LCA (life cycle assessment) was performed. The direct emission reduction was determined by the net power output. The environment impact on the cement production line was smaller for ORCs with the fluid of isohexane than that with the fluid of R601. When ORC was integrated with the cement production line, the reduction ratio of HTP was the largest but the reduction ratio of GWP was the smallest. This is because the reduction ratio of CO is the largest, followed by those of SO_2 and NO_x. The CO and SO_2 gases are the main pollutant of HTP. Fig. 19 shows the reduction ratios of EIL after ORC is integrated with the cement production line. The ORCs with fluids of R601 and R245fa had the largest (1.83%) and smallest (1.49%) reduction ratios, respectively.

4.5. Comparison with other studies and comments on the ORC applications

Table 9 summarized the related ORC economic and environmental analysis in the literature. There are three types of economic analysis of ORCs. The first type study regards the general applications of ORCs such as by Liu et al. [12]. Because the heat source is not specific, the analysis is suitable for the ORC system alone, not including the heat source information. The second type of economic studies is related to waste heat driven ORCs. The waste heat can be the flue gas from boiler, the cement production line (e.g.

Table 8
The weighting potential of the cement production line after introduction of ORC.

Working fluids	GWP ($PE_{China,90}$)	AP ($PE_{China,90}$)	EP ($PE_{China,90}$)	HTP ($PE_{China,90}$)
Hexane	0.158890	0.057958	0.032943	0.098006
Isohexane	0.158897	0.057967	0.032945	0.098022
R601	0.158804	0.057861	0.032919	0.097839
R123	0.158830	0.057886	0.032928	0.097881
R245fa	0.159084	0.058162	0.033004	0.098357

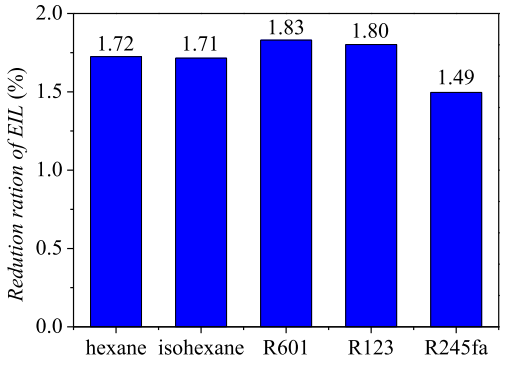

Fig. 19. The reduction ratio of EI.

Legmann [27]), etc. Because the fuel cost is not necessary, ORC applications in these areas have acceptable economic performance. Besides, ORCs apparently reduce the CO_2, SO_2 and NO_x emissions. The third type of studies concerns the renewable energy driven ORCs such as reported by Kosmadakis et al. [15] and Stoppato [28]. The PBP is relatively longer. The economic and environmental performance of ORCs should be further improved. This investigation shows that ORC application in the cement industry can achieve better economic and environmental benefits. This is because the fuel cost is not necessary and the maintenance cost is low. Most importantly, the waste heat is huge, making the possibility to apply large scale ORCs. The results in this paper are similar to those reported by Legmann [27]. In summary, small scale ORCs have poor economic and environmental performances. But the performance is improved with increases in the ORC capacity or scales.

Based on the NPV, PBP and LEC data, it is found that it is economic to introduce ORCs into the cement production line. The investment cost of ORCs is an important factor to be considered for such applications, which depend on the heat source such as the waste heat, solar energy and biomass energy, etc. The available experience demonstrates that larger scale ORC application is mature, but small scale ORC application is still in the infancy stage [29]. Expander is a key component in ORCs. Small scale expander needs further investigation. References [13,14] showed

Table 9
Related studies of ORC economic and environmental analysis in the literature.

Refs.	Industry sector or production line	ORC machine	Economic performance and environment impact	Comments or remarks
Liu et al. [12]	General treatment of waste heat, $T_{h,in}$ = 423.15 K, $m_{h,in}$ = 1 kg/s	Subcritical pressure ORC; organic fluids: R114, R245fa, R123, R601a, Pentane, R141b and R113; air cooling; Tube-shell heat exchangers; parameters: T_{amb} = 298.15 K, W_{net} = 9.2 −10.0 kW, η_s = 0.8, η_p = 0.75, life cycle of 20 years.	LCA evaluation method; EIL = 0.12–0.20 m $PE_{China,90}$; GWP had the most serious effect on the environment, accounting for 28.4–37.9% of the total EI.	ORC had less influence on environment with 1kWh electricity generation. It is noted that the influence of ORC on the environment should be analyzed by combining ORC with specific waster heat source.
Walsh et al. [13]	Low grade heat from stacks of a coke oven in steel production line, $T_{h,in}$ = 221 °C, $m_{h,in}$ = 66 kg/s	Subcritical pressure ORC; organic fluid of benzene; water cooling; parameters: η_{net} = 11%, W_{net} = 2.31 MW or 0.08 MJ/kg coke	The investment cost was 2023 €/kW; The annual running cost accounts for 4% of the total investment cost; PBP: 3–6 years; Annual CO_2 emission reduction of 10,927 t; The GWP reduction of 0.14%.	The PBP is relatively longer. For a single coke production line, the ORC had less effect on environment. But due to large percentage of the coke industry in UK, ORC can reduce CO_2 emission apparently.
Tchanche et al. [14]	waste heat, $T_{h,in}$ = 180 °C, $m_{h,in}$ 0.21 kg/s, $T_{h,out}$ = 67.25 °C	A of small-scale ORC prototype; Organic fluid of R245fa; water cooling; the expander modified from an oil-free scroll compressor; T_{amb} = 10 °C, P_{ev} = 11.84 bar, W_{net} = 2kWe, η_t = 8.23%; life cycle: 20years	Investment cost of 5775 €/kW; LEC = 13.27 c€/kWh; PBP = 6 years at the electricity cost of 20 c€/kWh. Alternatively; at 50kWe scale, investment cost = 3034 €/kW, LEC = 7 c€/kWh and PBP = 2.5years.	The studied small scale ORC has longer PBP. The application of large scale ORCs improves the economical performance.
Kosmadakis et al. [15]	solar thermal energy with $T_{h,in}$ = 130–140 °C, circulator = 12 m^3/h	Dual stage ORCs. High temperature section: R245fa fluid, W_t = 8.5 kW. Low temperature section: R134a fluid, W_t = 6.9 kW	The reverse osmosis desalination system had the cost of 1,85,712 €, with ORC covering 25.36% (44,572 €). The power cost was 2.74 €/kWh, fresh water cost was 6.85 €/m^3. The system PBP was 20 years.	The fresh water cost using solar-driven dual stage ORC approached to that of Photo Voltatic RO.
Legmann [27]	The grate cooler exhaust air in cement industry, $T_{h,in}$ = 275 °C, $T_{h,out}$ = 125 °C, air flow rate = 1,50,000Nm^3/h	Subcritical pressure ORC with pentane as the working fluid; air cooling; tube-shell heat exchanger; ORMAT turbine and W_{net} = 1.5 MW	The running and maintenance cost was about 0.002 $/kWh. The annul CO_2 emission reduction was 2.63% (about 7600 t).	From the running parameters after the 3.5 years operation of ORC in the cement production line, ORC had low maintenance cost and can reduce the emission to some degrees.
Stoppato [28]	Waste heat from a sawmill, $T_{h,in}$ = 310 °C, flow rate = 18,803Nm^3/h	ORC unit T1100 by Turbodens.r.l. company. The total heat input was 6.725 MW with W_{net} = 1.255 MW, η_{net} = 18.6% and W_{heat} = 5.35 MW.	The thermal energy cost was 0.03 €/kWh and the electricity cost was 0.14–0.27 €/kWh. The ORC consumed 2,11,28,040 −12,02,10,913 Nm^3 flue gas.	The economic performance of biomass energy driven ORC depends on the operation strategy of the power plant. The hybrid thermal-electricity supply plant substitutes the distributed boilers. The gas emission is far away from the users. But the gas emission is not apparently reduced except SO_x.

the specific cost of ORCs depends on the ORC power capacity (scale). The specific cost is decreased with increases in the ORC scales. Thus, it is concluded that the economic performance of ORC applied in the cement industry can be further improved if the scale is raised. It is known that in China, the investment costs are 4000 ¥/kW (468 €/kW) and 5500 ¥/kW (643.5 €/kW) for large scale coal-fired power plant and the gas power plant, respectively. These values are about 20–30% of the ORC power station. Thus, it is seen that the ORC economic performance should be further improved.

It is mentioned here that this study has some limitations. For example, the electricity price is assumed to be constant. But the electricity prices are different during peak and valley utilization periods. The base electricity price is 0.117 €/kWh, but it is increased and decreased by 50% during the peak and valley utilization periods, respectively. The PBP will be decreased if one prefers to operate ORCs during the valley electricity utilization period.

In addition to the above factors, the China policy will also influence the ORC economic performance. For example, as an energy saving award, 600 ¥ per one ton standard coal saving will be refunded to the company. Considering this factor, the PBP of ORC applied in the cement industry will be decreased to be shorter than one year, based on our estimation.

5. Conclusions

The ORC integrated with the China cement production line was investigated. The waste heat source is the dry air at the kiln cooler outlet with its temperature of 220 °C. Five working fluids of hexane, isohexane, R601, R123 and R245fa were selected for ORCs. These fluids are suggested based on the critical temperature criterion proposed by the authors' group recently. The ORC thermal efficiency, net power output and heat exchanger area are calculated. The NPV and PBP methods evaluated the economic performance. The LCA (life cycle assessment) evaluated the environment impacts combining the China's energy consumption data. The following conclusions can be drawn:

- For the 4000 t/d cement production line, ORCs could generate 67,85,540–81,21,650 kWh electricity per year, equivalent to save 2035–2436 tons standard coal and reduce 7743–9268 tons CO_2 emission.
- ORCs reduced gas emissions of CO_2 by 0.62–0.74%, SO_2 by 3.83–4.59% and NO_x by 1.36–1.63%.
- The payback period was from 2.74 to 3.42 years.
- The ORCs with the five working fluids had the reduction ratios of EIL by 1.49–1.83%, GWP by 0.74–0.92%, AP by 2.34–2.84%, EP by 0.96–1.22% and HTP by 2.38–2.89%.
- The ORC with R601 as the working fluid had the best economic performance and apparently gas emission reductions among those with the five working fluids.
- The ORCs integrated with the cement production line could have good economic performance and reduce the gas emissions apparently. The economic performance of ORCs applied in the cement industry will be further improved when the application scale is increased.

Acknowledgments

This work was supported by the Natural Science Foundation of China of International cooperation project (51210011), the Natural Science Foundation of China (51436004) and the 111 project (B12034).

References

[1] National Bureau of Statistics of China. China statistical yearbook 2013. Beijing: China Statistics Press; 2013 [in Chinese].
[2] Zhou F. The development and utilization of industrial waste heat resources brilliant future. Macroecon Manag 2012;9:43–4 [in Chinese].
[3] Zhuang C. The status and development trend of industrial waste heat utilization of cement. China Cem 2005;12:9–11 [in Chinese].
[4] Lakew AA, Bolland O. Working fluids for low-temperature heat source. Appl Therm Eng 2010;30(10):1262–8.
[5] Hung TC, Wang SK, Kuo CH, Pei BS, Tsai KF. A study of organic working fluids on system efficiency of an ORC using low-grade energy sources. Energy 2010;35(3):1403–11.
[6] Tchanche BF, Papadakis G, Lambrinos G, Frangoudakis A. Fluid selection for a low-temperature solar organic Rankine cycle. Appl Therm Eng 2009;29(11):2468–76.
[7] Dai Y, Wang J, Gao L. Parametric optimization and comparative study of organic Rankine cycle (ORC) for low grade waste heat recovery. Energy Convers Manag 2009;50(3):576–82.
[8] Roy JP, Misra A. Parametric optimization and performance analysis of a regenerative organic Rankine cycle using R-123 for waste heat recovery. Energy 2012;39(1):227–35.
[9] Wei D, Lu X, Lu Z, Gu J. Performance analysis and optimization of organic Rankine cycle (ORC) for waste heat recovery. Energy Convers Manag 2007;48(4):1113–9.
[10] Roy JP, Mishra MK, Misra A. Parametric optimization and performance analysis of a waste heat recovery system using organic Rankine Cycle. Energy 2010;35(12):5049–62.
[11] Zhang SJ, Wang HX, Guo T. Performance comparison and parametric optimization of subcritical organic Rankine cycle (ORC) and transcritical power cycle system for low-temperature geothermal power generation. Appl Energy 2011;88(8):2740–54.
[12] Liu C, He C, Gao H, Xie H, Li Y, Wu S, et al. The environmental impact of organic Rankine cycle for waste heat recovery through life-cycle assessment. Energy 2013;56:144–54.
[13] Walsh C, Thornley P. The environmental impact and economic feasibility of introducing an organic Rankine cycle to recover low grade heat during the production of metallurgical coke. J Clean Prod 2012;34:29–37.
[14] Tchanche BF, Quoilin S, Declaye S, Papadakis G, Lemort V. Economic feasibility study of a small scale organic Rankine cycle system in waste heat recovery application. In: ASME 2010 10th Biennial conference on engineering systems design and analysis. American Society of Mechanical Engineers; 2010. p. 249–56.
[15] Kosmadakis G, Manolakos D, Kyritsis S, Papadakis G. Economic assessment of a two-stage solar organic Rankine cycle for reverse osmosis desalination. Renew energy 2009;34(6):1579–86.
[16] Zhang D. New dry process cement production technology and new equipment introduction. Silicon Val 2008;22. 99–99.
[17] Zhang F. The application of cement kiln pure low temperature waste heat power generation organic Rankine cycle technology. Energy Sav Technol 2003;21(4):23–5.
[18] Engineering thermodynamics. Higher Education Press; 2001.
[19] Wang J, Zhang J, Chen Z. Molecular entropy, thermal efficiency, and designing of working fluids for organic Rankine cycles. Int J Thermophys 2012;33(6):970–85.
[20] Rayegan R, Tao YX. A procedure to select working fluids for solar organic Rankine cycles (ORCs). Renew Energy 2011;36(2):659–70.
[21] Kosmadakis G, Manolakos D, Kyritsis S, Papadakis G. Comparative thermodynamic study of refrigerants to select the best for use in the high-temperature stage of a two-stage organic Rankine cycle for RO desalination. Desalination 2009;243(1–3):74–94.
[22] Mikielewicz D, Mikielewicz J. A thermodynamic criterion for selection of working fluid for subcritical and supercritical domestic micro CHP. Appl Therm Eng 2010;30(16):2357–62.
[23] Kuo CR, Hsu SW, Chang KH, Wang CC. Analysis of a 50kW organic Rankine cycle system. Energy 2011;36(10):5877–85.
[24] Xu JL, Yu C. Critical temperature criterion for selection of working fluids for subcritical pressure organic Rankine cycles. Energy 2014;74C:719–33.
[25] Liu S, Lin Z. Study on life cycle assessment method of portland cement. Chin Environ Sci 1998;18(4):328–32 [in Chinese].
[26] Yang J, Xu C, Wang R. Product life cycle assessment and application. Meteorological Press; 2002 [in Chinese].
[27] Legmann H. Recovery of industrial heat in the cement industry by means of the ORC process. In: 44th Annual cement Industry Technical Conference. IEEE Cement Industry Technical Conf; 2002. p. 29–35.
[28] Stoppato A. Energetic and economic investigation of the operation management of an organic Rankine cycle cogeneration plant. Energy 2012;41:3–9.
[29] Vélez F, Segovia J, Martín M, Antolín G, Chejne F, Quijano A. A technical, economical and market review of organic Rankine cycles for the conversion of low-grade heat for power generation. Renew Sustain Energy Rev 2012;16:4175–89.

Glossary

A: *heat transfer area (m^2)*
C: *specific heat, kJ/kg K*

h:	specific enthalpy(kJ/kg)
K:	heat transfer coefficient (W/m^2 K)
$\dot{m}$:	mass flow rate (kg/s)
$\dot{Q}$:	heat rate (kW)
T:	temperature (K)
$\triangle T$:	temperature difference (K)
$\dot{W}$:	power (kW)

Greek symbols

η:	thermal efficiency
ε:	recuperation efficiency

Subscripts

air:	cooling air
air, in:	cooling air in
air, out:	cooling air out
amb:	ambient
cond:	condenser
cond, s:	the single-phase region of the condenser
cond, tw:	the two-phase region of the condenser
ev:	evaporator
ev,s:	the single-phase region of the evaporator
ev,tw:	the two-phase region of the evaporator
global:	global energy conversion
max:	maximum
min:	minimum
net:	net
r:	recuperation
s:	isentropic
t:	expander
tot:	total
wf:	working fluid
wh:	waste heat
wh, in:	heat carrier fluid of waste heat enters the ORC
wh, out:	heat carrier fluid of waste heat leaves the ORC
1–6:	state point
p:	pump/pressure
2s:	state point 2 for the ideal case
5s:	state point 5 for the ideal case

Acronyms

AP:	acidification potential
APR:	heat exchanger area per unit power output
EI:	environment impact
EIL:	environment impact load
EP:	eutrophication potential
GWP:	global warming potential
HTP:	human toxicity potential
LCA:	life cycle assessment
LEC:	levelized electricity cost
NPV:	net present value
NSP:	new suspension pre-heater
ODP:	ozone depletion potential
ORC:	organic Rankine cycle
PBP:	payback period